

Effect of Buffer Layer Design on Vertical GaN-on-GaN p-n and Schottky Power Diodes

Houqiang Fu, Xuanqi Huang, Hong Chen, Zhijian Lu, Xiaodong Zhang, and Yuji Zhao, *Member, IEEE*

Abstract— We study vertical GaN p-n and Schottky power diodes with different buffer layer thicknesses grown on free-standing GaN substrates, using metalorganic chemical vapor deposition. High breakdown voltage of > 1 kV and low specific on-resistance of $3 \text{ m}\Omega\cdot\text{cm}^2$ are achieved on GaN p-n diode with $1 \mu\text{m}$ buffer layer and $9 \mu\text{m}$ drift layer without passivation or field plate. Detailed device analysis on GaN Schottky diodes indicates that buffer layer has significant impacts on the electrical properties of drift layer and thus device performances of GaN p-n diodes. A thicker buffer layer will significantly enhance the breakdown voltages of these devices, which is possibly due to the improved material quality of drift layers with reduced defect densities. Higher doping concentration in drift layer with thicker buffer layer will, however, lower breakdown voltage. More discussions reveal improving the material quality of drift layer plays a more dominant role in achieving high breakdown GaN-on-GaN p-n and Schottky diodes with increasing buffer layer thickness.

Index Terms— Gallium nitride, p-n diodes, Schottky diodes, power electronics, buffer layer, drift layer, breakdown.

I. INTRODUCTION

WURTZITE III-nitride semiconductors have enabled a variety of applications including laser diodes (LDs) [1], light-emitting diodes (LEDs) [2]–[6], solar cells [7], photodetectors [8], [9] and high electron mobility transistors (HEMTs) [10]. Due to the advantages of low loss, low noise and low junction capacitance [11], GaN-based power diodes such as Schottky diodes and p-n diodes are also attractive for high power and high voltage applications. Conventional GaN power devices grown on foreign substrates such as Si and SiC, however, suffered from high defect densities ($> 10^9 \text{ cm}^{-2}$) in the materials, which significantly limit device performances [12], [13]. Recently, vertical GaN p-n power diodes grown on low defect density ($< 10^6 \text{ cm}^{-2}$) bulk GaN substrates have been demonstrated with promising performances such as high breakdown voltages and low on-resistance [14]–[18], where various device structures such as thicker drift layer, passivation and field plate have been proposed to further enhance the breakdown voltage of GaN p-n diodes. In addition to device structures, material

Manuscript received February 20, 2017; accepted April 2, 2017. Date of publication April 4, 2017; date of current version May 22, 2017. This work was supported by the Defense Threat Reduction Agency Young Investigator Award. The review of this letter was arranged by Editor Y. Wu. (Corresponding author: Yuji Zhao.)

The authors are with the School of Electrical, Computer, and Energy Engineering, Arizona State University, Tempe, AZ 85287 USA (e-mail: yuji.zhao@asu.edu).

Color versions of one or more of the figures in this letter are available online at <http://ieeexplore.ieee.org>.

Digital Object Identifier 10.1109/LED.2017.2690974

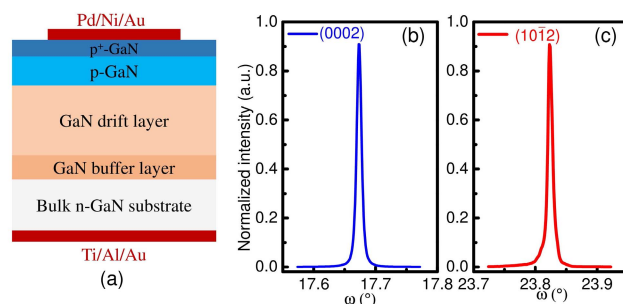


Fig. 1. (a) Schematic view of GaN p-n diodes grown on bulk GaN substrate with varying GaN buffer layer thickness using MOCVD. Rocking curve of (b) (0002) plane and (c) (10 $\bar{1}$ 2) plane for GaN p-n diodes by HRXRD.

properties such as defect density and doping concentration of device epilayers will also play a significant role in the performances of GaN p-n diodes. However, there are very few reports on this subject. In this work, we study the effect of buffer layer on the electrical properties of vertical GaN-on-GaN p-n and Schottky diodes.

II. GROWTH AND DEVICE FABRICATION

GaN p-n diodes were grown by conventional metalorganic chemical vapor deposition (MOCVD) on free-standing n-type GaN substrates ($\sim 10^{18} \text{ cm}^{-3}$) from Sumitomo Electric Industries Ltd. using dot core method [19]. The device structure consists of a n^+ -GaN buffer layer ($[\text{Si}] = 2 \times 10^{18} \text{ cm}^{-3}$ for all samples) with various thicknesses (50 nm, 400 nm, 1 μm , and 1 μm for samples A, B, C, and D), a 9- μm -thick unintentionally doped (UID) or lightly doped ($[\text{Si}] = 2 \times 10^{16} \text{ cm}^{-3}$ only for sample D) drift layer, a 500 nm p-GaN with Mg doping concentration of 10^{19} cm^{-3} , and a 20 nm heavily doped p^+ -GaN ($[\text{Mg}] = 10^{20} \text{ cm}^{-3}$). GaN buffer layers are grown at lower growth rate and temperature than drift layers and general information about growth methods can be referred to Nakamura *et al* [1].

Before fabrication, the samples were characterized by high resolution X-ray diffraction (HRXRD) measurement. Figure 1(b) and 1(c) show the representative (0002) symmetric and (10 $\bar{1}$ 2) asymmetric plane rocking curves (RCs) for the samples. The full width at half maximum (FWHM) of (0002) RCs are 30–60 arc sec and FWHM of (10 $\bar{1}$ 2) RCs are 20–30 arc sec. The dislocation density of the samples can be estimated using the following equation [19]: $D = \frac{\beta_{(0002)}^2}{9b_1^2} + \frac{\beta_{(10\bar{1}2)}^2}{9b_2^2}$, where β is FWHM and \vec{b} is the Burgers vector. All samples have a dislocation densities on the order of 10^6 cm^{-2} , which are significantly lower than that of typical GaN devices

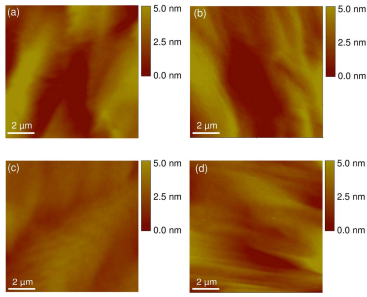


Fig. 2. AFM images ($10\ \mu\text{m} \times 10\ \mu\text{m}$) of (a) sample A, (b) sample B, (c) sample C, and (d) sample D.

grown on sapphire ($> 10^9\ \text{cm}^{-2}$). To further confirm the quality of epilayers, the surface roughness of as-grown samples were examined by Bruker's Dimension atomic force microscopy (AFM) in Fig. 2. The root-mean-square (RMS) roughness of $10 \times 10\ \mu\text{m}^2$ scanning area of the samples is found to be in the range of 0.5-1.5 nm, which is comparable to previous reports on bulk GaN substrate [21]–[23]. Both HRXRD and AFM results show that low-defect-density GaN epilayers with good surface morphology are obtained on bulk GaN substrates.

The GaN p-n diodes were fabricated using circular mesa with diameter ϕ of $260\ \mu\text{m}$ via inductively coupled plasma (ICP) etch with etching depth of $1.5\ \mu\text{m}$. No passivation or field plate (FP) were incorporated. For p-GaN ohmic contact ($\phi = 200\ \mu\text{m}$), Pd/Ni/Au metal stacks were deposited by electron beam evaporation and subsequently annealed in N_2 . P-contacts showed good ohmic behavior with a contact resistance of $8.6 \times 10^{-3}\ \Omega\cdot\text{cm}^2$ and sheet resistance of $33.3\ \text{k}\Omega/\text{sq}$, extracted by transmission line method (TLM) with two probes. For n-type ohmic contact, non-alloyed Ti/Al/Au stacks were formed at the backside of GaN substrates using electron beam evaporation. In addition, in order to study the electrical properties of the drift layers (i.e., material quality and doping concentration), Pd/GaN Schottky barrier diodes (SBDs) were also fabricated where Schottky contacts were directly formed on the drift layers without growing p-GaN and p⁺-GaN. Specifically, the SBDs have a n⁺-GaIn buffer layer ([Si] = $2 \times 10^{18}\ \text{cm}^{-3}$ for all samples) with various thicknesses (20 nm, 100 nm, 400 nm, and 400 nm for SBD1, SBD2, SBD3, and SBD4), a 9- μm -thick unintentionally doped (UID) or lightly doped ([Si] = $2 \times 10^{16}\ \text{cm}^{-3}$ only for SBD4) drift layer. The current–voltage (I–V) and capacitance–voltage (C–V) characteristics were measured using Keithley 4200-SCS parameter analyzer and Keithley 2410 sourcemeter at room temperature. The reverse breakdown measurements were conducted in Fluorinert liquid FC-70.

III. RESULTS AND DISCUSSIONS

Figure 3(a) shows the forward I–V characteristics and differential specific on-resistance R_{on} (dV/dI) for sample A, B, C and D. All p-n diodes exhibit good rectifying behaviors with a turn-on voltage of $\sim 3.1\ \text{V}$ and high on/off ratio $\sim 10^{10}$. The differences of on-current between four samples are not intrinsic to the devices and are likely due to inhomogeneous p-contact resistances [24]. Low R_{on} of $3\ \text{m}\Omega\cdot\text{cm}^2$ were obtained on all devices at 4 V. It's worth mentioning that all devices show similar R_{on} possibly due to large p-contact resistances despite different drift layer resistances of four samples. Furthermore, light emission was observed from all devices under high forward bias voltage. The measured

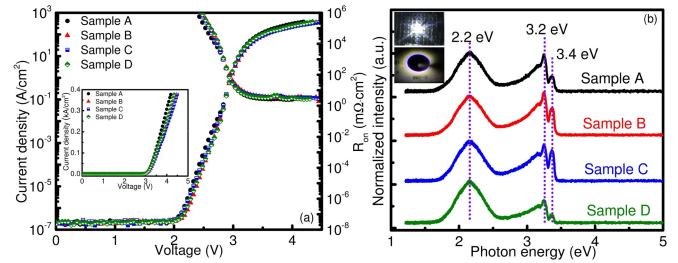


Fig. 3. (a) Forward I–V characteristics and differential specific on-resistance R_{on} of sample A (50 nm n⁺-GaIn buffer layer and $9\ \mu\text{m}$ UID GaN drift layer), B (400 nm n⁺-GaIn buffer layer and $9\ \mu\text{m}$ UID GaN drift layer), C (1 μm n⁺-GaIn buffer layer and $9\ \mu\text{m}$ UID GaN drift layer), and D (1 μm n⁺-GaIn buffer layer and $9\ \mu\text{m}$ n⁻-GaIn drift layer) in semilog scale. The insets are I–V curves in linear scale. (b) EL spectrum of four samples at forward bias of 4 V. The inset shows images of illuminated sample A and an individual device on it.

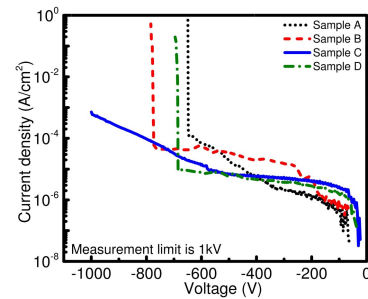


Fig. 4. Reverse I–V characteristics of sample A (50nm buffer, UID), B (400nm buffer, UID), C (1 μm buffer, UID) and D (1 μm buffer, n⁻-GaIn).

electroluminescence (EL) spectrum of the four samples at forward bias of 4 V was shown in Fig. 3(b). Three EL peaks at 2.2 eV, 3.2 eV and 3.4 eV were observed on all samples. The origin of these peaks are explained in detail by Qi *et al* [24]. The strong EL suggests the radiative recombination in GaN p-n diodes and is an indication of high material quality [24].

Figure 4 presents the reverse I–V characteristics of the four samples. The samples in order of decreasing breakdown voltage are: sample C (more than 1000 V) > sample B (772 V) > sample D (687 V) > sample A (647 V). Sample C with 1 μm buffer layer and $9\ \mu\text{m}$ UID drift layer shows the largest breakdown voltage. This result indicates that thicker GaN buffer layer can significantly enhance breakdown capability of GaN p-n diodes. Furthermore, the large difference in breakdown voltages between sample C and D also suggests that the doping concentration of the drift layer also plays a critical role in determining the breakdown voltage. The following analysis reveals that the improved breakdown capability of sample C is the result of better material quality due to thicker buffer layer and/or lower net doping concentration of drift layer.

To further study the electrical properties of the drift layers and their impacts on device performances of GaN p-n diodes, the GaN SBDs with the same drift layers were characterized by I–V and C–V measurements. Figure 5(a) shows the forward I–V characteristics of the four Pd/GaN Schottky diodes (SBD1, SBD2, SBD3 and SBD4) with diameter of $260\ \mu\text{m}$. Note GaN p-n diodes have similar forward current level on all samples as shown in Fig. 3(a) due to large p-contact resistance while forward current of SBDs is mainly determined by the metal/semiconductor (drift layer) interface. Therefore, the I–V characteristics of SBDs are directly related to the electrical

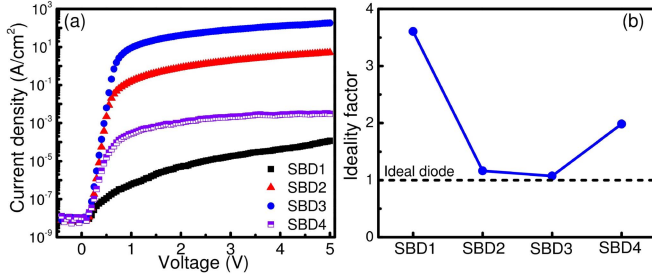


Fig. 5. (a) Forward I-V characteristics and (b) ideality factor of GaN Schottky diodes SBD1 (20 nm buffer layer and UID drift layer), SBD2 (100 nm buffer layer and UID drift layer), SBD3 (400 nm buffer layer and UID drift layer), and SBD4 (400 nm buffer layer and n⁻-GaN drift layer).

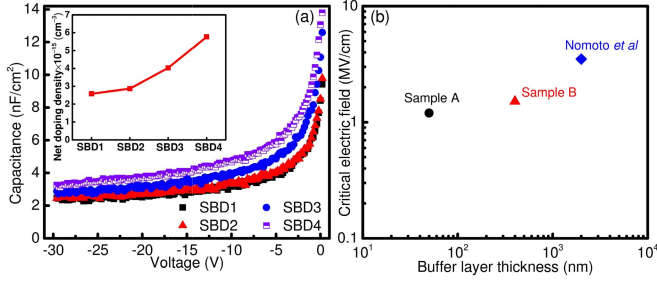


Fig. 6. (a) C-V characteristics of four GaN Schottky diodes. The inset shows the extracted net doping density for the four devices. (b) Comparison of critical electric field of p-n diodes with different buffer layer thicknesses.

properties of drift layers. Distinct on-currents are observed on different samples, which suggest that buffer layer thickness can dramatically alter the electrical properties of the drift layers. A near unity ideality factor of 1.07 was obtained for SBD3 as shown in Fig. 5(b), which signifies very high material quality of the drift layer [25]. With the same UID drift layer, the ideality factor decreases with increasing buffer layer thickness, indicating thicker buffer layer results in better material quality which can result from reduced defect density. This argument is also supported by the AFM data in Fig. 2. RMS of devices with thicker buffer layers are also smaller. In contrast, with the same buffer layer, higher drift layer doping concentration leads to larger ideality factor and therefore reduced material quality. These results showed thick buffer layer is required to improve the material quality of drift layers and achieve high breakdown voltage even though devices are grown on bulk GaN substrates.

Figure 6(a) shows C-V characteristics of the four Pd/GaN SBDs at a frequency of 1 MHz. The net doping concentration ($N_D - N_A$) can be extracted using Eq. (1):

$$N_D - N_A = -\frac{2}{q\epsilon_0\epsilon_r d \left(\frac{1}{C^2}\right)/dV} \quad (1)$$

where N_D is donor concentration, N_A is acceptor concentration, q is electron charge, ϵ_0 is permittivity of the vacuum, and ϵ_r is relative permittivity of GaN. After plotting $1/C^2$ vs V , a good linear relationship was obtained on all devices. The net doping concentrations of UID drift layers are in the range of 2×10^{15} to 4×10^{15} cm⁻³, which are comparable to that of recent reports on MOCVD grown GaN p-n diodes [15], [16], [25]. With nominal Si concentration of 2×10^{16} cm⁻³, a net doping concentration of 5.8×10^{15} cm⁻³ was determined, indicating a very low acceptor doping

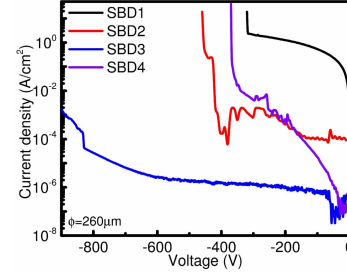


Fig. 7. Reverse I-V characteristics of four GaN Schottky diodes (SBD1, SBD2, SBD3 and SBD4) with mesa diameter of 260 μm.

concentration on the level of 10^{16} cm⁻³ [25]. It's also worth noting that the net doping concentration is increased for devices with thicker buffer layers, which is possibly related to charged defects [26]. With the net doping concentration obtained, critical electric field can be calculated in [16]:

$$V_{BD} = E_c t_{DR} - \frac{q(N_D - N_A)t_{DR}}{2\epsilon_0\epsilon_r} \quad (2)$$

where V_{BD} is the breakdown voltage, E_c is critical electric field, t_{DR} is thickness of drift layer. Figure 6(b) shows the critical electric fields of sample A and B in comparison with reported device with 2 μm buffer layer [16]. Devices with thicker buffer layer showed larger critical electric field, which is preferable for high breakdown devices. It should also be noted that the breakdown fields of our devices are relatively lower than that in Ref. 24 due to insufficient mesa isolation and larger contact diameter. The breakdown voltages of the GaN Schottky diodes were also measured in Fig. 7. The Schottky diodes showed the same trend as the p-n diodes (Fig. 4): thicker buffer layer can enhance the breakdown voltage while high doping concentration in drift layer can considerably reduce it.

Combining results from Fig. 4–7, we found that a thicker buffer layer can (1) not only contribute to better material quality which will enhance breakdown voltage, (2) but also result in a higher doping concentration in the drift layer which will reduce breakdown voltage. However, the highest breakdown voltages were still obtained on devices with thickest buffer layers (Sample C and SBD3). These results indicate material quality of a drift layer is more important than its doping concentration in achieving high breakdown voltage for the devices.

IV. CONCLUSION

We study the effect of buffer layer thickness on the electrical properties of vertical GaN-on-GaN p-n and Schottky diodes grown on free-standing GaN substrates. At forward bias, all diodes exhibit excellent rectifying behaviors with on/off ratio of $\sim 10^{10}$ and low R_{on} of 3 mΩ·cm². At reverse bias, thicker buffer layer can significantly enhance the breakdown voltage due to improved material quality of the drift layer possibly by reducing defect density. Breakdown voltage of over 1 kV were achieved. These results indicate that material quality is the key to achieving high breakdown on GaN p-n and Schottky diodes.

ACKNOWLEDGMENT

The samples were provided by IQE KC, LLC. The authors gratefully acknowledge the use of facilities within the LeRoy Eyring Center for Solid State Science at Arizona State University.

REFERENCES

- [1] S. Nakamura, G. Fasol, and S. J. Pearton, *The Blue Laser Diode: The Complete Story*, 2nd ed. Berlin, Germany: Springer, 2000, doi: 10.1007/978-3-662-04156-7.
- [2] Y. Zhao, S. Tanaka, C.-C. Pan, K. Fujito, D. Feezell, J. S. Speck, S. P. DenBaars, and S. Nakamura, "High-power blue-violet semipolar (2021) InGa_N/Ga_N light-emitting diodes with low efficiency droop at 200 A/cm²," *Appl. Phys. Exp.*, vol. 4, no. 8, p. 082104, Jul. 2011, doi: 10.1143/APEX.4.082104.
- [3] H. Fu, Z. Lu, X. Zhao, Y.-H. Zhang, S. P. DenBaars, S. Nakamura, and Y. Zhao, "Study of low-efficiency droop in semipolar (2021) InGa_N light-emitting diodes by time-resolved photoluminescence," *J. Display Technol.*, vol. 12, no. 7, pp. 736–741, Jul. 2016, doi: 10.1109/JDT.2016.2521618.
- [4] H. Chen, H. Fu, Z. Lu, X. Huang, and Y. Zhao, "Optical properties of highly polarized InGa_N light-emitting diodes modified by plasmonic metallic grating," *Opt. Exp.*, vol. 24, no. 10, pp. A856–A867, Apr. 2016, doi: 10.1364/OE.24.00A856.
- [5] C.-C. Pan, Q. Yan, H. Fu, Y. Zhao, Y.-R. Wu, C. Van de Walle, S. Nakamura, and S. P. DenBaars, "High optical power and low-efficiency droop blue light-emitting diodes using compositionally step-graded InGa_N barrier," *Electron. Lett.*, vol. 51, no. 15, pp. 1187–1189, Jul. 2015, doi: 10.1049/el.2015.1647.
- [6] H. Fu, Z. Lu, and Y. Zhao, "Analysis of low efficiency droop of semipolar InGa_N quantum well light-emitting diodes by modified rate equation with weak phase-space filling effect," *AIP Adv.*, vol. 6, no. 6, p. 065013, Jun. 2016, doi: 10.1063/1.4954296.
- [7] X. Huang, H. Fu, H. Chen, Z. Lu, D. Ding, and Y. Zhao, "Analysis of loss mechanisms in InGa_N solar cells using a semi-analytical model," *J. Appl. Phys.*, vol. 119, no. 21, p. 213101, Jun. 2016, doi: 10.1063/1.4953006.
- [8] H. Fu, Z. Lu, X. Huang, H. Chen, and Y. Zhao, "Crystal orientation dependent intersubband transition in semipolar AlGa_N/Ga_N single quantum well for optoelectronic applications," *J. Appl. Phys.*, vol. 119, no. 17, p. 174502, May 2016, doi: 10.1063/1.4948667.
- [9] H. Fu, H. Chen, X. Huang, Z. Lu, and Y. Zhao, "Theoretical analysis of modulation doping effects on intersubband transition properties of semipolar AlGa_N/Ga_N quantum well," *J. Appl. Phys.*, vol. 121, no. 1, p. 014501, Jan. 2017, doi: 10.1063/1.4972975.
- [10] Y.-F. Wu, D. Kapolnek, J. P. Ibbetson, P. Parikh, B. P. Keller, and U. K. Mishra, "Very-high power density AlGa_N/Ga_N HEMTs," *IEEE Trans. Electron Devices*, vol. 48, no. 3, pp. 586–590, Mar. 2001, doi: 10.1109/16.906455.
- [11] Y. Cao, R. Chu, R. Li, M. Chen, R. Chang, and B. Hughes, "High-voltage vertical Ga_N Schottky diode enabled by low-carbon metal-organic chemical vapor deposition growth," *Appl. Phys. Lett.*, vol. 108, no. 6, p. 062103, Feb. 2016, doi: 10.1063/1.4941814.
- [12] R. Chu, A. Corrion, M. Chen, R. Li, D. Wong, D. Zehnder, B. Hughes, and K. Boutros, "1200-V normally off Ga_N-on-Si field-effect transistors with low dynamic on-resistance," *IEEE Electron Device Lett.*, vol. 32, no. 5, pp. 632–634, May 2011, doi: 10.1109/LED.2011.2118190.
- [13] G. Simin, X. Hu, N. Ilinskaya, A. Kumar, A. Koudymov, J. Zhang, M. A. Khan, R. Gaska, and M. S. Shur, "7.5 kW/mm² current switch using AlGa_N/Ga_N metal-oxide-semiconductor heterostructure field effect transistors on SiC substrates," *Electron. Lett.*, vol. 35, no. 24, pp. 2043–2044, Nov. 2000, doi: 10.1049/el:20001401.
- [14] I. C. Kizilyalli, A. P. Edwards, H. Nie, D. Bour, T. Prunty, and D. Disney, "3.7 kV vertical Ga_N PN diodes," *IEEE Electron Device Lett.*, vol. 35, no. 2, pp. 247–249, Feb. 2014, doi: 10.1109/LED.2013.2294175.
- [15] I. C. Kizilyalli, T. Prunty, and O. Aktas, "4-kV and 2.8-mΩ-cm² vertical Ga_N p-n diodes with low leakage currents," *IEEE Electron Device Lett.*, vol. 36, no. 10, pp. 1073–1075, Oct. 2015, doi: 10.1109/LED.2015.2474817.
- [16] K. Nomoto, B. Song, Z. Hu, M. Zhu, M. Qi, N. Kaneda, T. Mishima, T. Nakamura, D. Jena, and H. G. Xing, "1.7-kV and 0.55-mΩ-cm² Ga_N p-n diodes on bulk Ga_N substrates with avalanche capability," *IEEE Electron Device Lett.*, vol. 37, no. 2, pp. 161–164, Feb. 2016, doi: 10.1109/LED.2015.2506638.
- [17] H. Ohta *et al.*, "Vertical Ga_N p-n junction diodes with high breakdown voltages over 4 kV," *IEEE Electron Device Lett.*, vol. 36, no. 11, pp. 1180–1182, Nov. 2015, doi: 10.1109/LED.2015.2478907.
- [18] K. Nomoto, Z. Hu, B. Song, M. Zhu, M. Qi, R. Yan, V. Protasenko, E. Imhoff, J. Kuo, N. Kaneda, T. Mishima, T. Nakamura, D. Jena, and H. G. Xing, "Ga_N-on-Ga_N p-n power diodes with 3.48 kV and 0.95 mΩ-cm²: A record high figure-of-merit of 12.8 GW/cm²," in *IEDM Tech. Dig.*, Dec. 2015, pp. 971–974, doi: 10.1109/IEDM.2015.7409665.
- [19] K. Motoki, R. Hirota, T. Okahisa, and S. Nakahata, "Single crystal Ga_N substrate, method of growing single crystal Ga_N and method of producing single crystal Ga_N substrate," U.S. Patent 7087114, Aug. 8, 2006.
- [20] T. Ide, M. Shimizu, X. Q. Shen, K. Jeganathan, H. Okumura, and T. Nemoto, "Improvement of film quality using Si-doping in AlGa_N/Ga_N heterostructure grown by plasma-assisted molecular beam epitaxy," *J. Crystal Growth*, vol. 245, nos. 1–2, pp. 15–20, Nov. 2002, doi: 10.1016/S0022-0248(02)01665-2.
- [21] C. Hemmingsson, P. P. Paskov, G. Pozina, M. Heuken, B. Schineller, and B. Monemar, "Growth of bulk Ga_N in a vertical hydride vapour phase epitaxy reactor," *Superlattices Microstruct.*, vol. 40, nos. 4–6, pp. 205–213, Oct. 2006, doi: 10.1016/j.spmi.2006.09.014.
- [22] T. Detchprohm, M. Zhu, Y. Li, Y. Xia, C. Wetzel, E. A. Preble, L. Liu, T. Paskova, and D. Hanser, "Green light emitting diodes on α -plane Ga_N bulk substrates," *Appl. Phys. Lett.*, vol. 92, no. 24, p. 241109, Jun. 2008, doi: 10.1063/1.2945664.
- [23] F. Xie, H. Lu, D. J. Chen, X. Q. Xiu, H. Zhao, R. Zhang, and Y. D. Zheng, "Metal-semiconductor-metal ultraviolet avalanche photodiodes fabricated on bulk Ga_N substrate," *IEEE Electron Device Lett.*, vol. 32, no. 9, pp. 1260–1262, Sep. 2011, doi: 10.1109/LED.2011.2160149.
- [24] M. Qi, K. Nomoto, M. Zhu, Z. Hu, Y. Zhao, V. Protasenko, B. Song, X. Yan, G. Li, J. Verma, S. Bader, P. Fay, H. G. Xing, and D. Jena, "High breakdown single-crystal Ga_N p-n diodes by molecular beam epitaxy," *Appl. Phys. Lett.*, vol. 107, no. 23, p. 232101, Dec. 2015, doi: 10.1063/1.4936891.
- [25] Z. Hu, K. Nomoto, B. Song, M. Zhu, M. Qi, M. Pan, X. Gao, V. Protasenko, D. Jena, and H. G. Xing, "Near unity ideality factor and Shockley-Read-Hall lifetime in Ga_N-on-Ga_N p-n diodes with avalanche breakdown," *Appl. Phys. Lett.*, vol. 107, no. 24, p. 243501, Dec. 2015, doi: 10.1063/1.4937436.
- [26] D. Cherns and C. G. Jiao, "Electron holography studies of the charge on dislocations in Ga_N," *Phys. Rev. Lett.*, vol. 87, no. 20, p. 205504, Oct. 2001, doi: 10.1103/PhysRevLett.87.205504.